Relating Deformation to Hot Spots in Shock-Loaded Crystals of Ammonium Perchlorate

Harold W. Sandusky,* Brian C. Glancy,* and Dorn W. Carlson†
Naval Surface Warfare Center, Silver Spring, Maryland 20903
Wayne L. Elban‡
Loyola College, Baltimore, Maryland 21210
and
Ronald W. Armstrong§
University of Maryland, College Park, Maryland 20742

The purpose of this work is to perform a microscopic-scale study of the role that crystal defects have in forming hot spots during shock loading of large, optical quality, pure single crystals of ammonium perchlorate (AP). The crystals were immersed in mineral oil at various distances from a detonator that provided the shock. The small explosive donor permitted recovery of the crystals for quantitative chemical analysis of decomposition and microindentation hardness testing. Hardness testing was also performed on an unshocked crystal to determine 1) the slip systems associated with primary and secondary deformation in accommodating the indenter and 2) the crack propagation directions at the surface as well as into the crystal. High-speed photographs of the shock-loaded crystals showed slip and cracking systems identified by hardness testing. Some of the systems were luminous. In addition, when a crystal with a large indentation was shocked near its reaction threshold, significant light appeared in the vicinity of the identation following shock passage. As such, preferred chemical reactivity in AP has been associated with its deformation systems and the presence of large strain centers.

Introduction

A NUMBER of years ago, the formation of "hot spots" was proposed and experimentally verified as occurring in energetic materials in response to mechanical forces, such as those from impact.[1] Circumstances where hot spots occur suggest that their origin is closely connected to the microstructure and allied deformation properties of the energetic material. There is also experimental evidence indicating that crystalline explosives have microstructural properties that influence their shock sensitivity. This was observed on a macroscopic scale by Green and James[2] in small-scale gap tests on cyclotetramethylenetetranitramine (HMX) formulations made from crystals of differing quality. For pentaerythritoltetranitrate (PETN), Dick[3] determined that microscopic damage from gamma radiation enhanced the shock sensitivity of single crystals over that of relatively defect-free crystals. In addition, the shock sensitivity of the latter crystals was a function of orientation, indicating that shock-induced defects depend on the lattice arrangement.[4] To date, however, no work has been reported that spatially relates sites of microstructural imperfection to enhanced chemical reactivity as an energetic material is impacted or shocked.

The present study is a beginning effort to determine the role of material microstructure in chemical reactivity and dynamic deformation of single crystals of energetic materials subjected to shock. The results of high-speed photographs are integrated with material property measurements and chemical analyses, both of which were performed before and after shocking the crystals. Ammonium perchlorate (AP) was chosen for this study, in part because of its widespread use as a crystalline oxidizer ingredient in solid propellants and explosives. In addition, the thermal decomposition behavior of AP is well-understood, and its dislocation-based deformation behavior has been studied to some extent by other investigators,[5,6] providing valuable reference information for current deformation studies.

In drop-weight impact tests of a variety of materials reported by Heavens and Field,[7] AP ignited coincident with a sharp drop in its pressure-time curve, much like the result for cyclotrimethylenetrinitramine (RDX). Armstrong, et al.[8] developed a dislocation pile-up avalanche model to describe the localized heating associated with such discontinuous load drop behavior. The model has led to determining the presence of internal obstacles to dislocation pile-ups in RDX crystals[9] and to a comparison of pile-up characteristics in RDX and magnesium oxide (MgO) crystals.[10] There is difficulty, however, in predetermining a potential hot-spot site. For pressed compacts of AP crystals with 13% porosity, Macek and Durfee[11] determined the threshold for shock-induced reaction by measuring the weight loss of sealed samples that had been impacted by a gun projectile (velocities from 250–700 m/s). Relative to RDX, HMX, and PETN explosive crystals, local reaction sites in AP are more likely to quench without destroying the crystal. This suggests the feasibility of studying, perhaps on a microscopic scale, the role that crystal defects have in forming hot spots and in enhancing the shock reactivity of AP.

Experimental Approach

Large (>1 cm), optical quality, pure single crystals of AP were provided by T. L. Boggs, Naval Weapons Center, China Lake, California. The crystals had been grown for combustion studies, one of which is described in Ref. 12. AP has an orthorhombic unit cell with a crystal density of 1.95 g/cm^3. The drawing in Fig. 1 is for a typical cleaved crystal, showing size and shape along with cleavage surfaces and major crystallographic directions. The plastic deformation and fracture behaviors of AP were investigated by putting diamond pyramid (Vickers) microindentations into the (210) and (001)

Received Nov. 11, 1989; revision received Aug. 10, 1990; accepted for publication Sept. 10, 1990. This paper is declared a work of the U.S. Government and is not subject to copyright protection in the United States.

*Research Mechanical Engineer, Detonation Physics Branch.
†Research Chemist, Synthesis and Formulations Branch.
‡Associate Professor, Department of Electrical Engineering and Engineering Science.
§Professor, Department of Mechanical Engineering.

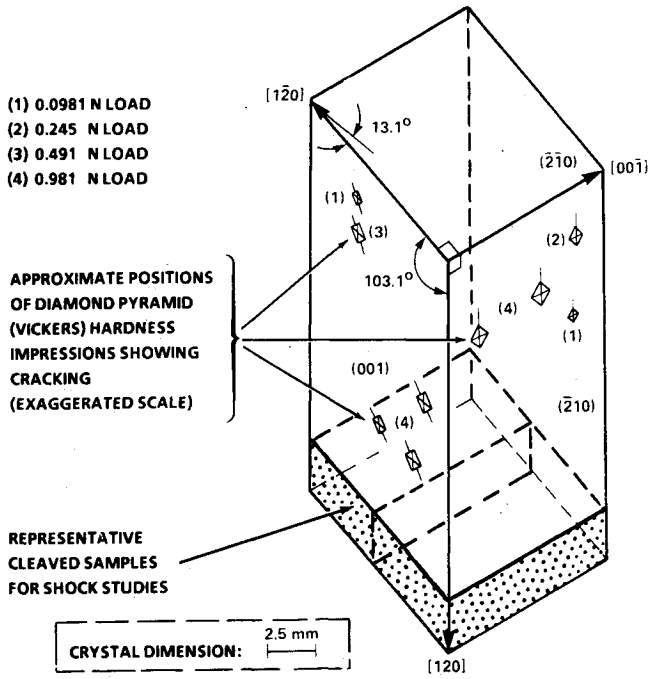

Fig. 1 Scale drawing of cleaved AP single crystal used in microindentation hardness tests.

cleavage surfaces of the crystal as shown in Fig. 1.[13] Hardness results on the (001) surface will be emphasized in order to relate to shock-loading observations obtained for the same surface.

graphic directions. The plastic deformation and fracture behaviors of AP were investigated by putting diamond pyramid (Vickers) microindentations into the ($\bar{2}$10) and (001) cleavage surfaces of the crystal as shown in Fig. 1.[13] Hardness results on the (001) surface will be emphasized in order to relate to shock-loading observations obtained for the same surface.

Shock experiments[13] were conducted on relatively small crystals of AP (<0.5 g) that were cleaved from a larger crystal as indicated, for example, in Fig. 1. Each crystal was immersed in mineral oil and shocked by a detonator (Reynolds RP-80) at a known separation distance. The Reynolds RP-80 uses an exploding bridgewire to initiate 78 mg of PETN, which in turn initiates 124 mg of RDX with binder. In the particular type of RP-80 that was used, the explosive components are in a Delrin sleeve that does not cover the output end of the detonator; that end was sealed from the oil with a light coat of Duco cement. Thus, the detonator was much like a small donor charge with little confinement. The experiments were confined in a 0.9-l steel chamber that had windows for photography and illumination (Fig. 2). Both a rotating mirror streak camera and an Imacon electronic camera have been used with backlighting from an electronic flash. The crystal either rested on a piece of oil-soaked polyurethane foam or was supported above a piece of foam by tape (0.05-mm thickness). This arrangement allowed recovery of the crystal for subsequent chemical analysis and hardness testing without obstructing the view of the camera. About 100 mg of most recovered samples were analyzed by liquid ion chromatography for the concentrations of Cl^-, ClO_3^-, NO_2^-, and NO_3^-.

The shock experiments were calibrated for peak pressure in the oil vs distance from the detonator (Fig. 3). In a separate experiment, a rotating mirror streak camera was used to precisely measure shock position vs time, which was differentiated to obtain shock velocity. A Hugoniot for heavy mineral oil, density, ρ_o, of 0.87 g/cm^3, was reported for the range of 15–150 kbar ($U = 2.18 + 1.53u$, where "U" is the shock velocity and "u" is the particle velocity, both in units of mm/μs).[14] Since pressures of less than 15 kbar were of interest, this Hugoniot was extrapolated to the 1.45 mm/μs sound velocity, c_o, for mineral oil with the equation

$$U/c_o = 1.503 - 0.503 \exp(-5\, u/c_o) + 1.53\, u/c_o$$

using an approach similar to that described previously.[15] With that modified Hugoniot and the experimental measurements of U, shock pressures in the oil were calculated using the jump equation, P_{oil} (kbar) = $10\rho_o Uu$. The AP Hugoniot used for matching the shocks in the oil and the crystal was $U = 2.84 + 1.6u$. A reported Hugoniot, $U = 2.84 + 2u$,[16] is consistent with a 2.84 mm/μs bulk sound speed in AP;[17] however, shock data for pressed AP (1.92 g/cm^3) at 155 and 178 kbars[18] were best fit with a slope of 1.6 in the U vs u relationship.

Microindentation Studies (Unshocked Crystal)

Micrographs of a Vickers impression (100 gf = 0.981 N load) in the (001) surface appear in Fig. 4. A Vickers hardness number (VHN) of 11 kgf/mm^2 (108 MPa) for that impression indicates that AP is soft, only ⅓ to ½ as hard as the molecular explosive RDX, using the result of various researchers as previously discussed.[10] The transmitted light micrograph in

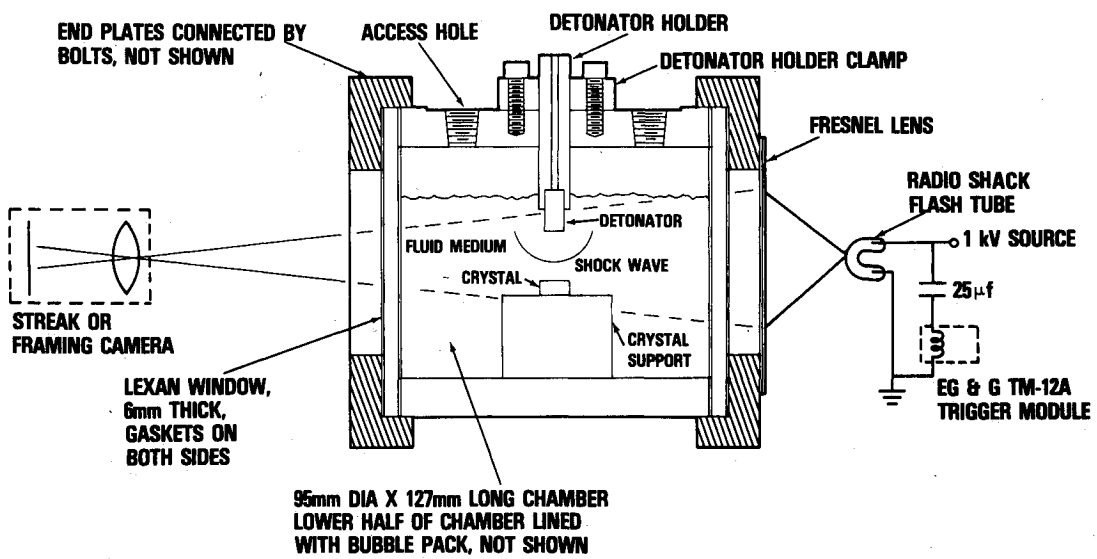

Fig. 2 Closed chamber for photography of shock reaction in small samples.

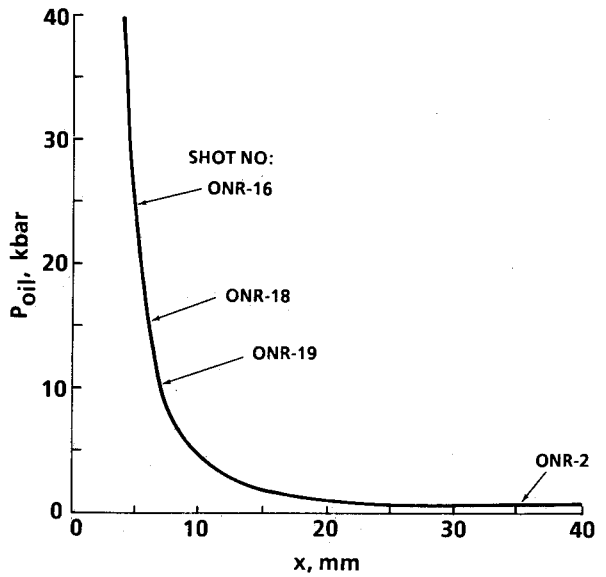

Fig. 3 Calibration of peak shock pressure in mineral oil vs distance from the detonator.

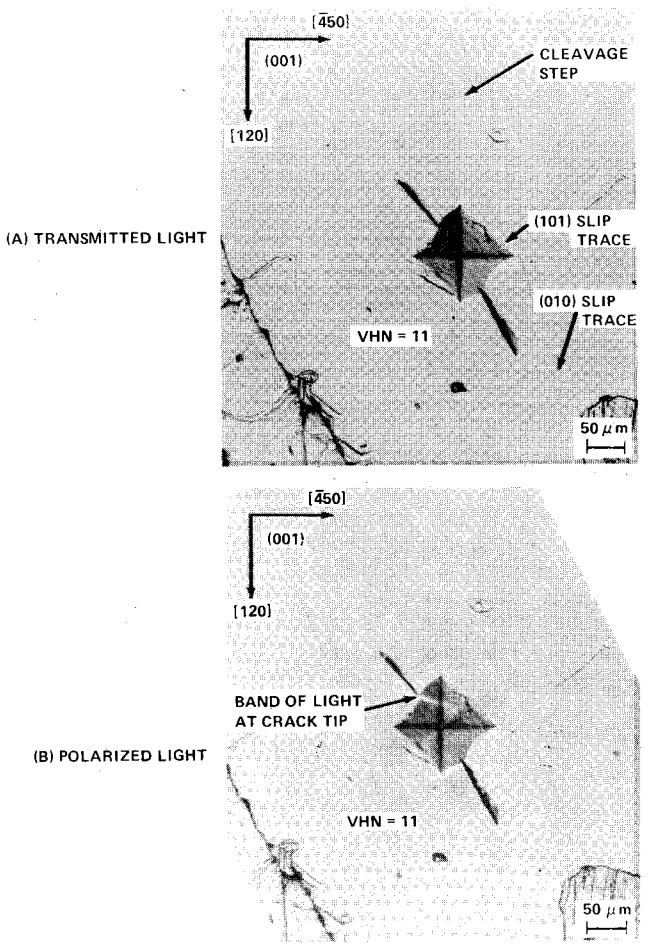

Fig. 4 Diamond pyramid (Vickers) hardness impression in (001) surface of AP.

Fig. 4a shows that the four facets of the impression have a distorted fourfold rotational symmetry. Large cracks emanate from two sides of the impression; beginning at a load of 500 gf (4.91 N), a second set of cracks in other indented AP crystals was observed with traces in the (001) surface approximately orthogonal to those in Fig. 4. The indentation was viewed in polarized light with the cross polarizers oriented to provide maximum extinction (Fig. 4b). The most obvious feature is a bright, sharply focused band of light near the impression at the tip of one of the cracks. This suggests that considerable strain energy is stored in the vicinity of this crack tip. Transmitted cross-polarized light was also observed close to the corners of the hardness impression. However, there was a surprising absence of transmitted light in the surrounding region away from the hardness impression. Rotating the AP crystal about the [001] direction between the cross polarizers did not appear to alter this finding. This observation suggests that the strain energy around the residual impression is relatively localized, although plastic deformation has occurred around the impression. When the (001) impression was viewed in transmitted light that was partially obstructed before the light entered the crystal (Fig. 5), prominent troughs were observed to emanate from two facets of the impression.

The indentation-forming (primary deformation) and volume-accommodating (secondary deformation) slip systems were identified for the (001) surface by performing a single-trace analysis utilizing, as much as possible, slip-system information reported previously.[5,6] The results of the analysis are presented in the stereographic projection that appears in Fig. 6. Subsequently, the results were confirmed by a two-trace analysis of slip lines formed at a spherical indentation placed near to the edge of the (001) surface of another crystal. The prominent troughs in Fig. 5 along $\pm$[010] are attributed to primary deformation on the $\pm$(010)[001] slip system. As such, it is concluded that this slip system is the easiest operating system in AP. Secondary deformation slip traces, appearing twin-like, are crossing bands within the troughs. These bands are attributed to apparent $\pm$(101)[001] slip-system activity orthogonal to the primary deformation system. The case where both slip systems are orthogonal to the indented surface is admittedly highly unusual but occurs because of the limited slip systems available. Limited systems is a contributing factor to the observation that initial cracking (i.e., at low loads) occurs (Fig. 5) in the region of greatest plastic deformation for the impression. The occurrence of cracking in AP where the deformation is greatest has been confirmed for Vickers indentations put into a ($\bar{2}$10) surface.[13]

The effect of indenter force on indentation diagonal length for Vickers indentations put into the (001) surface has been determined for forces ranging from 10 gf to 1.5 kgf (0.0981–14.7 N) (Fig. 7). Several additional crystals were studied, including some used in shock-loading experiments to be described later. The diametral size of radial cracks emanating

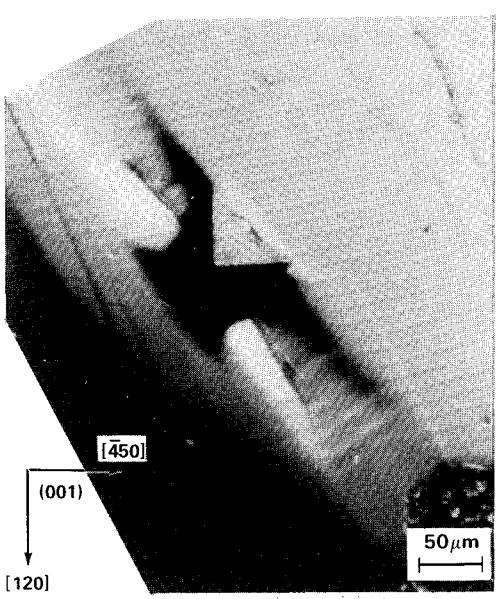

Fig. 5 Surface relief at Vickers hardness impression in (001) surface of AP.

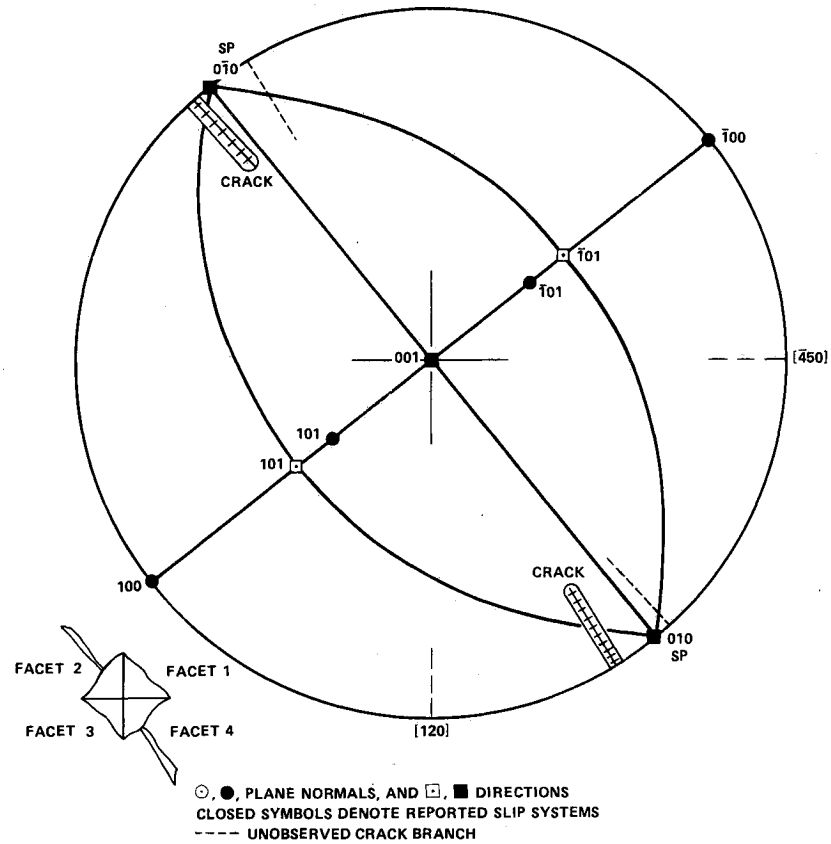

Fig. 6 Deformation systems for Vickers hardness impression in (001) surface of AP.

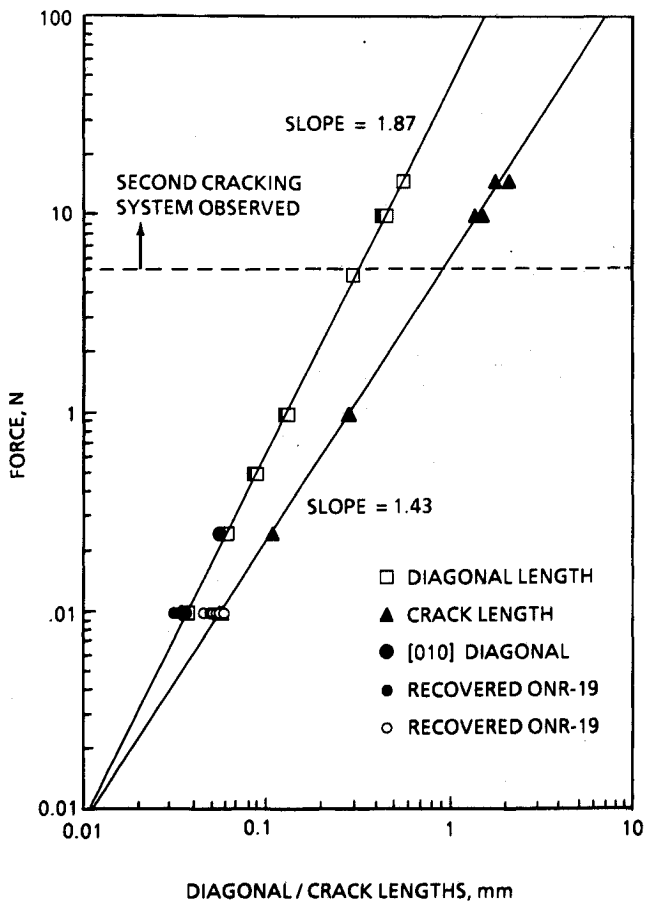

Fig. 7 Force vs diagonal and crack lengths for diamond pyramid (Vickers) impressions in (001) surface of AP ([120] or [1$\bar{2}$0] diagonal).

nearly along ±[010] was also measured for some of the indentations. The hardness was observed to decrease with increasing force; an exponent of 1.87 was obtained for the power-law dependence of indenter force on diagonal length. The exponent would be 2.0 for a constant value of hardness. The decrease in hardness is attributed to the occurrence of cracking. An exponent of a little less than 1.5 obtained for the force dependence on diametral crack length correlates well with indentation fracture-mechanics analyses developed by other researchers as previously discussed.[10] In this work, those indentations that exhibited the second cracking system were excluded from the least-squares analysis to determine the crack length exponent. The cracking apparently causes at least a partial strain energy release to occur due to dislocations escaping at the crack surfaces, thus yielding the reduced hardness values.

A release of strain energy would explain the relative absence of transmitted light observed at hardness indentations in the (001) surface when viewed using transmitted polarized-light microscopy. The release of strain energy in AP because of cracking is also an important consideration in the shock-reactivity work to be described below. A comparison of shock-reactivity behavior has begun for AP crystals with and without Vickers identations in the (001) cleavage surface. The desired enhanced shock reactivity at indentation sites would appear to be suppressed because of strain-energy dissipation. With respect to hazards assessments, an initial comparison between AP and RDX was made of their ability to dissipate strain energy by cracking.[19]

Shock-Loading Studies

The results of shock experiments over a range of 1–38 kbar are summarized in Table 1. Even at the highest shock pressures, most of each crystal was recovered for further analysis. The recovery of an intact crystal that was positioned only 7.0 mm from the detonator (P_{AP} = 16.7 kbar, Shot ONR-19) can

Table 1 Results from shocking AP crystals in mineral oil

Mineral Oil			AP Crystal		Chemical Analysis, ppm			
Shot ONR-	gap, mm	P_{oil}, kbar	P_{AP}, kbar	Recovered condition	Cl^-	NO_2^-	NO_3^-	ClO_3^-
Not shocked, Vickers indentation					420	8	46	4
2	35	0.6	1.0	No damage	600	8	29	25
3	23	1.0	1.8	No damage	530	12	38	22
4	15	2.0	3.5	No damage	410	18	39	10
5	8.2	7.2	11.6	Broke into 5 pieces	520	20	45	20
19	7.0	10.5	16.7	Intact but cloudy (Figs. 11–13)	Saved for hardness tests (Fig. 7)			
Vickers indentation; high-speed photographs in Fig. 10								
17	6.0	15.5	24.4	Broke into two pieces	Two separate analyses:			
					1400	6	60	—
					900	18	20	20
18	6.0	15.5	24.4	Broke into small pieces	Analysis failed			
Vickers indentation; high-speed photographs in Fig. 9								
16	5.0	24.8	38.5	Large pieces were 88% of original weight	11,000	8	46	4
High-speed photographs in Fig. 8								

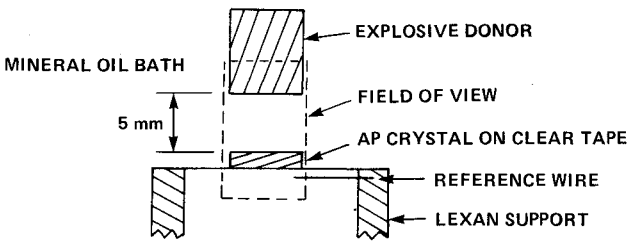

RELATIVE TIME FOR EACH FRAME LISTED IN MICROSECONDS

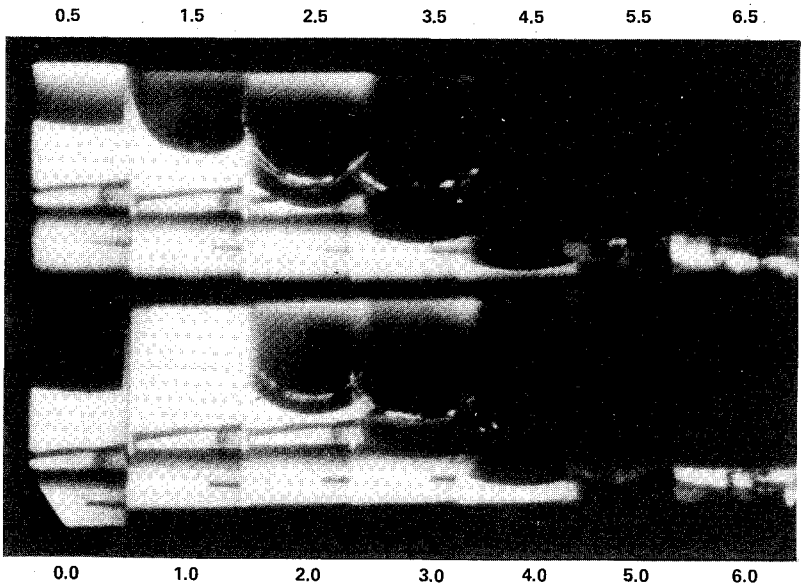

DESCRIPTION OF EVENTS SEEN IN INDIVIDUAL FRAMES

0.0 μs NO ACTION
0.5 μs LUMINOUS DETONATION WAVE PROPAGATING IN EXPLOSIVE
1.0 μs LUMINOUS DETONATION WAVE AT END OF EXPLOSIVE DONOR
1.5 μs EXPLOSIVELY DRIVEN SHOCK JUST ENTERING MINERAL OIL
2.0 μs SHOCK WAVE APPROACHING CRYSTAL; LUMINOUS DETONATION PRODUCTS SEEN JUST BEHIND SHOCK WAVE
2.5 μs SHOCK WAVE ENTERING AP CRYSTAL; SMALL ZONE OF WEAK LUMINOSITY AT CRYSTAL/OIL INTERFACE
3.0 μs SHOCK WAVE JUST COMPLETED PASSAGE THROUGH CRYSTAL; DETONATION PRODUCTS NOW IMPINGING ON UPPER SURFACE

SUBSEQUENT FRAMES MOSTLY OBSCURED BY DETONATION PRODUCT GASES

Fig. 8 Backlit framing camera record of an AP crystal being shocked at 24 kbar (Shot ONR-16).

be contrasted with the pulverizing of another crystal that was not immersed in oil but separated by the same distance from the detonator with a plastic (PMMA) gap. The chromatography measurements revealed a large increase in only the Cl^- concentration as shock pressure increased. Based on those measurements, the threshold of shock reaction for a relatively defect-free crystal in this arrangement was ~25 kbar (shock pressure in the crystal, P_{AP}). With the baseline established for the onset of reactivity in a "good" crystal, several experiments were performed on crystals with a macroscopic defect created at the surface by the hardness indenter. High-speed framing camera records were obtained of the shock interaction with crystals in Shots ONR-16 through ONR-19; Shots ONR-18 and ONR-19 each had a 1000 gf (9.81 N) Vickers hardness impression in the (001) surface of the crystal.

At the highest shock pressure (Shot ONR-16), the photographs in Fig. 8 show that the shock was still quite curved when entering the crystal and that the gas bubble from the expanding detonation products, which are opaque to the backlighting, reached the crystal shortly after the shock. The shock curvature and the additional gas bubble loading both would have contributed to the breakup of the crystal. The shock fronts were luminous in the two crystals with P_{AP} = 24.4 kbar (Shots ONR-17 and 18). In the second experiment (ONR-18), the top of the crystal was blackened with permanent ink to reduce any light originating from hot detonator products, in case that had contributed to the luminosity of the shock front. The crystal in Shot ONR-18 was located with the as-viewed (001) surface under the center of the detonator, whereas in other experiments the crystal was centered under the detonator. The photographs in Fig. 9 show the luminous front as well as a luminous band in the vicinity of the indentation. The luminous band first appeared in the 0.6-μs frame (approximately corresponding to the time interval required for the shock to pass the indentation) and then moved from right to left across the crystal. The band was observed to be particularly intense and straight in the 1.4-μs frame. The linearity of the light band suggests that it is crystallographic in origin. The angle between the band and the [120] direction was measured to be 2 deg less than the analogous determination for the trace of the bottom crack at the hardness impression in Figs. 4 and 5. This is the crack that extends from facet 4 of the impression as designated in the insert appearing in Fig. 6. Even though the crack trace at the impression is wavy at the higher magnification in Figs. 4 and 5, associating the band of light with this crack seems plausible because of its inclination to the (001) surface. It is important to note that the sense of the inclination requires that Figs. 4 and 5 be rotated 180 deg about [001] in order that they properly correspond with Fig. 9 as viewed. Then, the observed right-to-left movement of the light band would logically be attributed to this crack propagating away from the viewer more deeply into the crystal.

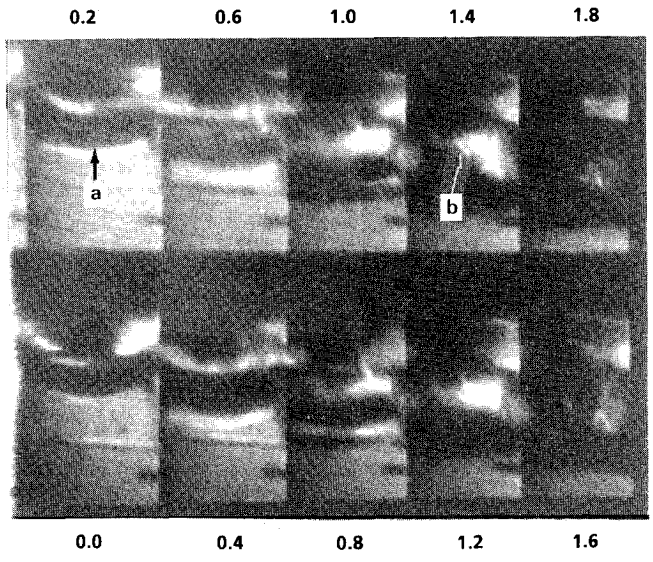

Fig. 9 Backlit framing camera record of an AP crystal being shocked at 16 kbar (Shot ONR-18).

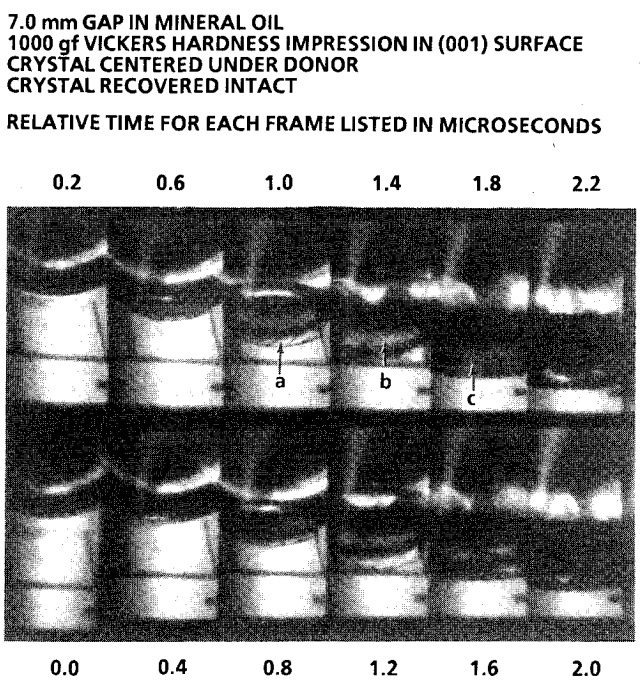

Fig. 10 Backlit framing camera record of an AP crystal being shocked at 13 kbar (Shot ONR-19).

At the somewhat lower shock pressure (P_{AP} = 16.7 kbar) in Shot ONR-19, the shock front in the crystal appeared as a distinct dark line (Fig. 10). Thus, the luminous fronts in the previous experiments were probably a response of the crystal and not an optical effect from the backlighting. Between the shock front in Shot ONR-19 and the interaction of the shock with the as-viewed (001) surface, crystallographic-appearing diagonal lines in an otherwise clear region appeared, beginning in the 0.6-μs frame. These diagonal lines occurred in only one basic direction and not also in the normally expected complementary direction. Similar observations for Shots ONR-17 and 18 were probably obscured by the luminous shock fronts that were present. Further behind the shock front, most clearly seen in the 1.4-μs frame, there was a region of partial transmittance of the backlighting where many closely spaced diagonal lines appeared.

The angular relationships between various diagonal lines and the [120] direction were measured for Shot ONR-19 (Fig. 10). Following shock passage, the prominent diagonal line in the 1.8-μs frame was determined to coincide with an (010) trace to within 1 deg. During shock passage in the 1.0-μs frame, the angular deviation from being an (010) trace varied from 4–15 deg ($\pm$2 deg uncertainty). This deviation occurs in the correct rotational direction when attributed to shock

compression. However, the magnitude of the rotation caused by uniaxial straining is estimated to be only 2 deg. Optical distortion in the shock to mineral oil is believed to be responsible for the remaining deviation. As such, the diagonal lines are believed to be associated with the (010)[001] slip system, the readily observable secondary (volume-accommodating) deformation system described earlier for the Vickers indentation.

As indicated in Table 1, the sample in Shot ONR-19 was recovered intact. The photograph of the recovered crystal in Fig. 11 shows that the top surface was concave as a result of the spherically expanding shock from the detonator and the crystal became somewhat cloudy in appearance. Microscopic examination of the previously indented (001) surface revealed numerous, closely spaced straight lines, indicating that extensive slip-trace formation had occurred (Fig. 12). These traces were narrow, resembling the appearance of slip traces surrounding a Vickers impression in an unshocked crystal. Furthermore, the traces were found to be orthogonal to one another and were identified as (010) and ($\bar{1}$00) slip planes (Fig. 13). By comparison, the bands attributed to (010) slip during shock loading in (Fig. 10) were wider, possibly because of the nonuniform distortion associated with the curved shock front. There is also the apparent contradiction that no ($\bar{1}$00) slip planes were visible during shock loading. Either the (100) slip planes resulted and did not successfully block the transmitted light, or ($\bar{1}$00) slip predominantly occurred during unloading of the shock pressure.

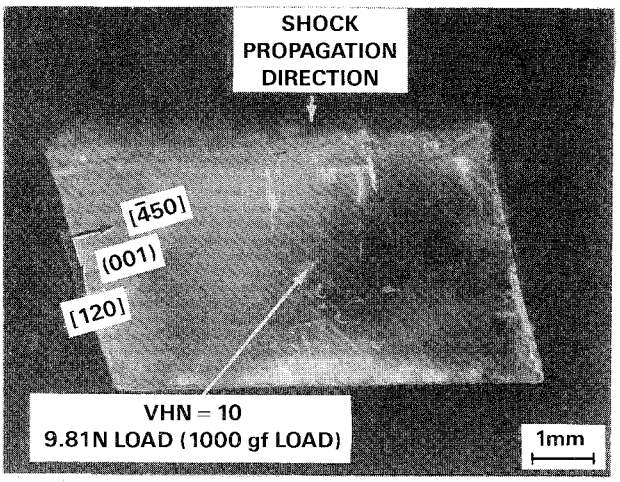

Fig. 11 (001) surface of shocked AP crystal from Shot ONR-19 showing large hardness impression.

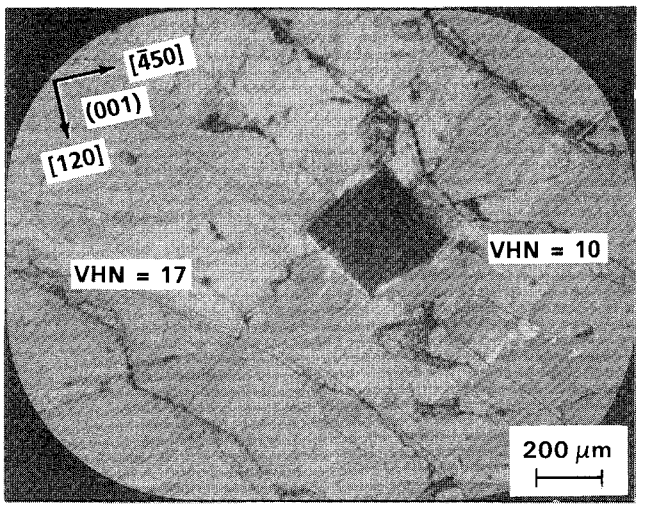

Fig. 12 Reflected light photomicrograph of (001) surface of shocked AP crystal (Shot ONR-19) showing original and subsequent Vickers hardness impressions and extensive slip-trace formation.

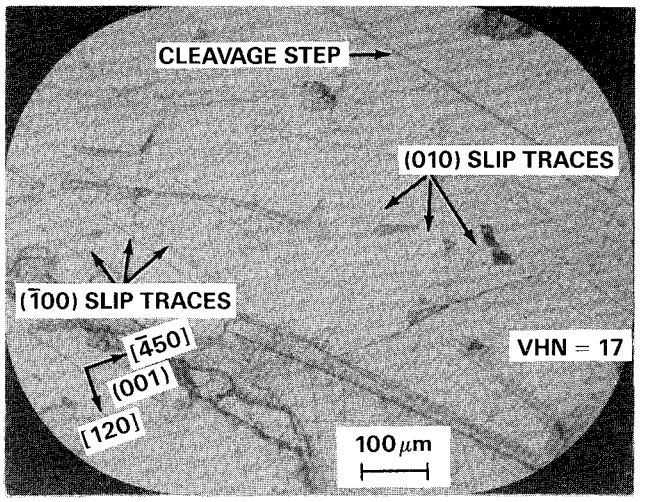

Fig. 13 Reflected light photomicrograph of (001) surface of shocked AP crystal (Shot ONR-19) showing numerous ($\bar{1}$00) and (010) slip traces.

The curved shock waves in the crystals should act like a high-rate ball indentation whose penetration into the crystal is limited. Relative to the (001) surface of observation in Fig. 11, the nonplanar shock produced an orthogonal stress component out of the crystal surface. The stress direction was opposite to that produced by an indentation in the (001) surface. Despite the opposite loading directions, similar slip traces should be expected for the two cases. This association reveals an advantage of having curved shocks in the present study.

Vickers microindentation hardness testing was performed on the crystal that had been recovered in Shot ONR-19 to determine changes in microstructure occurring as a result of shock loading. A series of 10 gf (0.0981 N) indentations were put into various areas of the (001) surface of the recovered crystal. The hardness and cracking properties changed depending on the location of the indentation, and the measurements are included in Fig. 7. The largest change in hardness (VHN = 19 vs 14 for a separate unshocked crystal tested at 10 gf) occurred in the region of the crystal that first experienced shock-wave passage. Referring to Figs. 12 and 13, a VHN of 17 was measured at the orthogonal intersection of slip traces near to the 1000 gf indentation (VHN = 10) made prior to shock loading. The hardness in other regions of the crystal away from the 1000 gf indentation increased by ~7%. The accompanying radial crack extension was also measured for each of the 10-gf indentations. These measurements were compared to the average of two determinations obtained for 10-gf indentations put into the (001) cleavage surface of an unshocked crystal described previously.[13] Crack extension in the shocked crystal was found to be reduced generally, with differences ranging from −18 to +5%.

Summary and Conclusions

Initial results have been obtained for the roles that deformation, fracture, and material microstructure have on the shock reactivity of AP. Optical quality crystals of AP were shocked by a small explosive donor over a pressure range of 1–38.5 kbar, while immersed in mineral oil. The threshold for reaction in this arrangement was 25 kbar for relatively defect-free crystals, as determined by liquid ion chromatography on recovered pieces. Over a pressure range of 16.7–38.5 kbar, high-speed photography was used to view the (001) surface of several crystals during shock loading. Two of the crystals had a large surface defect created by a diamond pyramid (Vickers) indenter. The high-speed photographs of the shocked crystals showed, although not in each experiment, a

luminous shock front, distinct diagonal lines immediately behind the front that were attributed to the (010)[001] slip system, a moving luminous band that appeared to be a propagating crack, and light in the vicinity of a surface indentation presumably due to chemical reaction. Near the reaction threshold, it appears that reaction in even a relatively defect-free crystal is inhomogeneous, being directly related to its material microstructure. Other investigators have recently shocked RDX crystals at much higher pressures, ~100 kbar, and observed light which they attribute to crystal deformation.[20]

Surface traces of slip planes and cracks associated with forming Vickers hardness impressions in the (2̄10) and (001) cleavage surfaces of an unshocked crystal were crystallographically identified. Slip systems were determined, the easiest operative system being (100)[001]. Particularly noteworthy is the observation that cracking occurs in the region of greatest plastic deformation. The effect of indenter force on indentation and resultant crack sizes was investigated for Vickers indentations put into the (001) surface. The hardness was observed to decrease with increasing force, which was attributed to the occurrence of cracking.

Acknowledgments

This work was supported by the Office of Naval Research under work request numbers N00014-87-K-0175 and N00014-85-WR-24103 as a cooperative effort between Loyola College, Baltimore, and the Naval Surface Warfare Center (NAVSWC), White Oak, including collaboration with the University of Maryland, College Park. Drs. Sigmund J. Jacobs and Richard R. Bernecker, NAVSWC, provided many helpful comments and guidance concerning the direction of the research. Dr. Donald A. Keefer, Loyola College, and Dr. Xian Jie Zhang, University of Maryland, College Park, helped with the micrographs in Figs. 4 and 5. Dr. Paul J. Coyne, Jr., Loyola College, developed a computer program that generated the stereographic projection appearing in Fig. 6. Dr. David S. Richards, Loyola College, helped with the analysis and preparation of Fig. 7.

References

[1]Bowden, F. P., and Yoffe, A. D., *Fast Reactions in Solids*, Butterworths Scientific Publications, London, 1958, Chapter 5, pp. 57–87.

[2]Green, L. G., and James, E., Jr., "Radius of Curvature Effect on Detonation Velocity," *Fourth Symposium (International) on Detonation*, Office of Naval Research, Dept. of the Navy, Washington, D.C., ACR-126, 1965, pp. 86–91.

[3]Dick, J., "Plane Shock Initiation of Detonation in γ-Irradiated Pentaerythritol Tetranitrate," *Journal of Applied Physics*, Vol. 53, No. 9, 1982, pp. 6161–6167.

[4]Dick, J., "Effect of Crystal Orientation on Shock-Initiation Sensitivity of Pentaerythritol Tetranitrate Explosive," *Applied Physics Letters*, Vol. 44, No. 9, 1984, pp. 859–861.

[5]Herley, P. J., Jacobs, P. W. M., and Levy, P. W., "Dislocations in Ammonium Perchlorate," *Journal of the Chemical Society*, Sec. A, No. 3, 1971, pp. 434–440.

[6]Williams, J. O., Thomas, J. M., Savintsev, Y. P., and Boldyrev, V. V., "Dislocations in Orthorhombic Ammonium Perchlorate," *Journal of the Chemical Society*, Sec. A, No. 11, 1971, pp. 1757–1760.

[7]Heavens, S. N., and Field, J. E., "The Ignition of a Thin Layer of Explosive by Impact," *Proceedings of the Royal Society of London*, Series A., Vol. 338, No. 1612, 1974, pp. 77–93.

[8]Armstrong, R. W., Coffey, C. S., and Elban, W. L., "Adiabatic Heating at a Dislocation Pile-up Avalanche," *Acta Metallurgica*, Vol. 30, No. 12, 1982, pp. 2111–2116.

[9]Elban, W. L., Armstrong, R. W., Yoo, K. C., Rosemeier, R. G., and Yee, R. Y., "X-Ray Reflection Topographic Study of Growth Defect and Microindentation Strain Fields in an RDX Explosive Crystal," *Journal of Materials Science*, Vol. 24, No. 4, 1989, pp. 1273–1280.

[10]Armstrong, R. W., and Elban, W. L., "Cracking at Hardness Microindentations in RDX Explosive and MgO Single Crystals," *Materials Science and Engineering*, Series A., Vol. 111, 1989, pp. 35–43.

[11]Macek, A., and Durfee, R. L., *A Study of Energy Release in Rocket Propellants by a Projectile Impact Method*, NASA Contractor Rept. 66395, Atlantic Research Corp., Alexandria, VA, June 1967.

[12]Boggs, T. L., Zurn, D. E., and Netzer, D. W., "Ammonium Perchlorate Combustion: Effects of Sample Preparation; Ingredient Type; and Pressure; Temperature and Acceleration Environments," *Combustion Science and Technology*, Vol. 7, No. 4, 1973, pp. 177–183.

[13]Elban, W. L., Coyne, P. J., Jr., Sandusky, H. W., Glancy, B. C., Carlson, D. W., and Armstrong, R. W., "Investigation of the Origin of Hot Spots in Deformed Crystals: Studies on Ammonium Perchlorate and Reference Inert Materials," Naval Surface Warfare Center, Dahlgren, VA, NSWC MP 88-178, April 1988.

[14]Netherwood, P., and Tauber, D., "The Shock Hugoniot of Mineral Oil," Ballistic Research Lab., Aberdeen, MD, BRL MR 2214, Aug. 1974.

[15]Woolfolk, R. W., Cowperthwaite, M., and Shaw, R., "A 'Universal' Hugoniot for Liquids," *Thermochimica Acta*, Vol. 5, No. 4, 1973, pp. 409–414.

[16]Martynyuk, V. F., Khasainov, B. A., Sulimov, A. A., and Sukoyan, M. K., "Estimating Heat Production in the Detonation of Poured-Density Ammonium Perchlorate," *Combustion, Explosion, and Shock Waves*, Vol. 23, No. 1, 1987, pp. 58–60.

[17]Dobratz, B. M., and Crawford, P. C., (eds.), *LLNL Explosives Handbook*, Lawrence Livermore National Laboratory, Livermore, CA, UCRL-52997, Dec. 1985, pp. 7–37.

[18]Salzman, P. K., Irwin, O. R., and Anderson, W. H., "Theoretical Detonation Characteristics of Solid Composite Propellants," *AIAA Journal*, Vol. 3, No. 12, 1965, pp. 2230–2238.

[19]Elban, W. L., Coyne, P. J., Jr., Sandusky, H. W., Glancy, B. C., Carlson, D. W., and Armstrong, R. W., "Microindentation and Shock-Loading Studies on Single Crystals of Ammonium Perchlorate," *Proceedings of the ONR Workshop on Energetic Material Initiation Fundamentals*, Vol. I, Chemical Propulsion Information Agency Publication 516, Johns Hopkins University, Laurel, MD, 1988, pp. 608–637.

[20]Forbes, J. W., Tasker, D. G., Granholm, R. H., and Gustavson, P. K., "Direct Observation of Shocked Explosive Crystals Immersed in Liquids," *Shock Compression of Condensed Matter—1989*, edited by S. C. Schmidt, J. N. Johnson, and L. W. Davidson, Elsevier Science Publishers, Amsterdam, B. V., 1990, pp. 709–712.